Coupled Systems Mechanics, *Vol. 7, No. 3 (2018) 297-319*
DOI: https://doi.org/10.12989/csm.2018.7.3.297

Using structural intensity approach to characterize vibro-acoustic behavior of the cylindrical shell structure

Yuran Wang[a], Rong Huang[b] and Zishun Liu[*]

International Center for Applied Mechanics,
State Key Laboratory for Strength and Vibration of Mechanical Structure,
Shaanxi Engineering Research Center of Nondestructive Testing and Structural Integrity Evaluation,
Xi'an Jiaotong University, Xi'an, 710049, China

(Received April 29, 2017, Revised November 14, 2017, Accepted November 15, 2017)

Abstract. In this paper, the vibro-acoustic behaviors of vibrational cylindrical shells are investigated by using structural intensity approach. The reducing interior noise method for vibrating cylindrical shells is proposed by altering and redistributing the structural intensity through changing the damping property of the structure. The concept of proposed novel method is based on the properties of structural intensity distribution on cylindrical shells under different load and damping conditions, which can reflects power flow in the structures. In the study, the modal formulas of structural intensity are developed for the steady state vibration of cylindrical shell structures. The detailed formulas of structural intensity are derived by substituting modal quantities, in which the effect of main parameters such as weight coefficients and distribution functions on structure intensity are analyzed and discussed. Numerical simulations are first carried out based on the structural intensity analytical solutions of modal formulas. Through simulating the coupling vibration and acoustical radiation problems of cylindrical shell, the relationship between vibro-acoustic and structural intensity distribution is derived. We find that for cylindrical shell, by properly arranging damping conditions, the structural intensity can be efficiently changed and further the noise property can be improved. The proposed methodology has important implications and potential applications in the vibration and noise control of fuselage structure.

Keywords: cylindrical shell; noise control; structural intensity; vibro-acoustic

1. Introduction

It is an important subject and key issue in many engineering areas to understand the vibro-acoustic behaviors of vibrational structures. For example, the reduction of interior/exterior noise and vibration levels is a primary concern in automobiles and aircraft industries. In last few decades, many approaches and methodologies (Liu *et al.* 2005, Wang *et al.* 2005, Wang *et al.* 2017, Zhao *et al.* 2017) for efficiently controlling and reducing the vibration and noise levels in

∗Corresponding author, Professor, E-mail: zishunliu@mail.xjtu.edu.cn
[a]Postgraduate Student, E-mail: black.gundam@stu.mail.xjtu.edu.cn
[b]Research Assistant, E-mail: ronghuang@xjtu.edu.cn

http://www.techno-press.org/?journal=csm&subpage=8 ISSN: 2234-2184 (Print), 2234-2192 (Online)

equipment and carrier have been proposed, as people are finding themselves on the receiving end of noise pollution and needing more comfort environments. Generally speaking, reducing the levels of vibration and noise of thin-walled enclosures structures are broadly classified into active and passive control methods, and each one has advantages and disadvantages. The elastic, thin-walled cylindrical shell is an important type of engineering structure, such as: tubes, columns, airplanes and many others which can be simplified to this type of structure. Hence, understanding the vibro-acoustic behavior of the thin-walled cylindrical shell is imperative for a satisfactory design of this class of structures and there have several studies focusing on vibration analysis of thin-walled cylindrical structures (Javed *et al.* 2016). From their analysis, we know the interior noise in thin-walled cylindrical shell structures is mainly caused by vibrations of the shells, especially for low frequency vibrations of the shell. This structural-borne noise is due to the coupling between the structural vibration and the interior fluid or air. Therefore, the effective noise control can be achieved by reducing the vibration levels of the structures (Wu and Zhou 2016, Huang and Tseng 2008, Chesnais *et al.* 2017). The extensive reviews of the literature on passive and active structural vibro-acoustic control for suppressing enclosure cavity interior noise have been carried out by many researchers (Thompson 1989, Huang and Chen 2000). As the effectiveness of passive approach is limited, the research of active control techniques have be promoted in last few decades. For thin-walled cylindrical shell structures, the active structural noise control has been widely used to reduce low frequency sound transmission. Active structural acoustic control involves secondary structural input such as mechanical shakers or actuators applied directly to the enclosure structures. With this control method, structural actuators are integrated on the structural surfaces or walls in such a way as to modify and cancel the vibration of the panels of enclosure and thus reduce the noise radiation/transmission. This active vibration noise cancellation approach can offer improved performance that can augment other methods to significantly reduce internal noise level.

To ensure efficient noise reduction of vibrational structures, one needs to determine effective locations of dampers, sensors and actuators that installed on the structures. How to properly optimize the locations and values of dampers and actuators is the key issue for interior noise control of enclosure structures. There are few publications (Sommerfeldt 1993, Alfredsson 1993, Audrain *et al.* 2004, Liu *et al.* 2006, Murakami *et al*. 2010), which had discussed the control strategy for this active noise control and it is been mentioned the determination of damper locations can lead the improved control of the structural field. However, this technique has not been clearly demonstrated and extended to the cylindrical structures in previous research. In this paper, we will propose an efficient method for characterize the vibro-acoustic behaviors of cylindrical shell structures by adopting Structural Intensity (SI) approach.

This paper will introduce an approach, which can be applied to reducing the levels of vibration and noise of the cylindrical shell structure. The appraisal of the structural power flow and vibration shape is an important method in vibration and acoustic control. Structural intensity research is a new trend in the vibration analysis of structures. When a structure is exciting, the propagation of vibrational energy through the structure is related to the results of interaction between the stress and the velocity, which means the structural intensity, and it can reflect the structure power flow.

The concept of structural intensity was introduced firstly as a quantifier for the structural vibro-acoustic analysis in 1970s by Noiseux (1970). Structural intensity can be expressed as the resultant of stress and the velocity, which is a direction sum of the scalar product of the force vectors and their corresponding velocity vectors. Structural intensity is the power flow per unit cross-sectional area in plate and shell structures and a result of vibration. Pavic (1976) developed the formulation

of structural intensity. Verheij (1980) presented the cross spectral density method to measure the structural power flow in beams and pipes. Hambric (1990) developed the computational approach of structural intensity through the finite element method. Gavric and Pavic (1993) evaluated the structural intensity fields of a rectangular plate by using the computational approach and identified the source and the sink of the energy flow. Gavric *et al.* (1997) further extended modal superposition method in an experimental approach. Li and Lai (2000) calculated the structural intensity and surface mobility for a thin plate with viscous damper and structural damping. Williams (1991) investigated structural intensity in thin cylindrical shells. Xu, X.D *et al.* (2005) and Liu *et al.* (2005) first introduced the structural intensity streamline concept based on plate structures. Furthermore, Liu *et al.* (2005) theoretically derived the formulations for structural intensity streamline according to the concept of fluid mechanics streamline. The structural intensity streamline can be used to clearly display the structural intensity flow paths. Structural intensity streamline which represent the spatial distribution of the structural power flow can be visualized to show the positions of energy sources and sinks. After that, the structural intensity streamline concept was introduced into different engineering applications, such as the area of impact problem (Liu *et al.* 2005), snoring study in biomechanics (Liu *et al.* 2007), fracture mechanics and noise control etc. In noise control aspect, Liu *et al.* (2006) use structural intensity approach to propose a basic method of active and passive interior noise control for box structures.

This research is a further extension of previous works and it uses structural intensity method to study the vibro-acoustic behaviors of cylindrical shell structures. In this paper, we first theoretical derived the structural intensity formulas of cylindrical shell structures. Based on structural intensity general expression, a vibration mode method to calculate the structural intensity of cylindrical shell structures is proposed, which can be used to efficiently evaluate the structural intensity by introducing the vibration modes. Furthermore, the vibro-acoustic behaviors are investigated for cylindrical shell structures. This paper investigates the structural power flow in the cylindrical shell structure and studies the vibro-acoustic coupling for sound radiation using the structural intensity vector and streamline patterns. According to structural intensity characteristics of cylindrical shell, a new method for structural intensity distribution control is proposed by changing exciting and damping conditions. The proposed method could be used to reduce interior noise in the cylindrical shell structures.

This paper contains five parts. In section 2, the primary theory of structural intensity concept is reviewed and discussed. In this section we derived structural intensity formulations of cylindrical shell structures. The relationship of structural intensity and acoustic intensity of cylindrical shell is also provided. In section 3, according to the proposed formulations, the analytical solutions and numerical simulations of cylindrical shell are performed. From analytical and simulation results, some methods for controlling and altering structural intensity distribution are discussed. As an application example, the interior noise and vibro-acoustic behavior of the cylindrical shell which represent simplified fuselage structures are briefly described in section 4. Finally, the concluding remarks are provided in section 5.

2. Preliminary theory and formulation

2.1 Instantaneous and steady structural intensity

Analogous to the concept of acoustic intensity in acoustic medium, the structure power flow

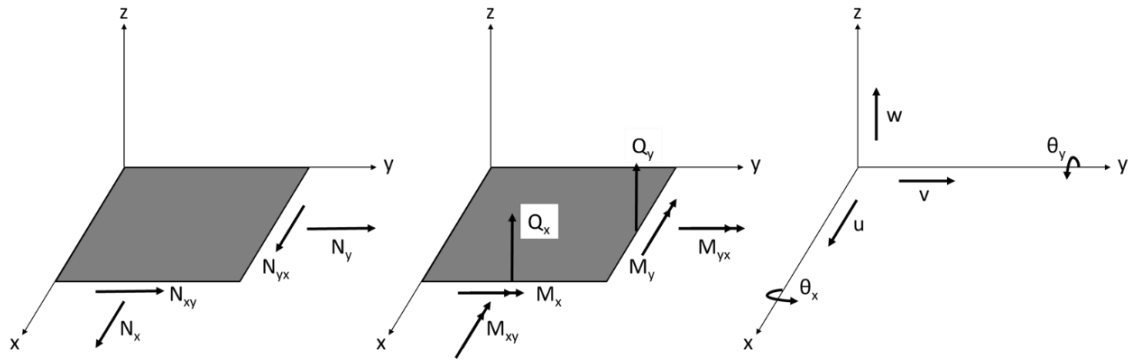

Fig. 1 Plate and shell element with forces and displacements

through per unit cross section area of a vibrational structure is defined as the structural intensity. The structural intensity can be expressed as the result of stress and the velocity, a scalar product of the force vectors and their corresponding velocity vectors. The instantaneous structural intensity component in the time domain can be defined as (Gavric and Pavic 1993)

$$i_k(t) = -\sigma_{kl}(t) v_l(t), \quad k,l = 1,2,3 \tag{1}$$

where $v_l(t)$ is the lth component of the velocity vector and $\sigma_{kl}(t)$ is the *kl*th component of the stress tensor, there are both functions of time.

The average of time mean of the *k*th instantaneous structural intensity component can be defined as

$$I_k = \langle i_k(t) \rangle, \tag{2}$$

where $\langle ... \rangle$ denotes time average.

For a steady state vibration, the steady structural intensity component in the frequency domain can be defined as

$$I_k(\omega) = -(1/2)\,\mathrm{Re}\left[\tilde{\sigma}_{kl}(\omega)\tilde{v}_l^*(\omega)\right], \quad k,l = 1,2,3 \tag{3}$$

where the superscript ~ and * denote complex number and complex conjugate respectively, *Re* denotes real part. The $\tilde{\sigma}_{kl}(\omega)\tilde{v}_l^*(\omega)$ is the function of cross-spectral density between stress and velocity components.

Finally, the integration of the steady structural intensity in the whole frequency domain equals the temporal mean of the instantaneous structural intensity

$$I_k = \langle i_k(t) \rangle = \int_\omega I_k(\omega), \tag{4}$$

2.2 Structural intensity in thin plates and cylindrical shells

With the development of the structural intensity concept and its application, specific formulations of structural intensity in plates and shells are given in form of displacements and

velocities, which can be easily measured. The computation of spatial derivatives of structural displacements and velocities are obtained by using analytical and finite element methods.

The computation of structural intensity in plates was calculated by Gavric and Pavic (1993) and Gavric *et al.* (1997). And the state of stress vectors distribution over the thickness of the thin plate can be expressed by the stress resultants at the mid plane of the thin plate. When it comes to the shell structure, since the stress resultants for the shell elements include the shear forces, the membrane forces, the bending moments and the twisting moments at the mid plane should be expressed as shown in Fig. 1. After the stress resultants integral along the thickness of the thin shell elements, we can derive that the structural intensity in terms of stress resultants is the net power flow per unit width. To sum up, velocities corresponding to the moments are the angular velocities and velocities corresponding to the forces are the in plane and transverse velocities, respectively.

When we solve flat thin plate problems under bending condition, membrane forces usually can be ignored. However, when it comes to the thin cylindrical shell structure, membrane forces must be taken into consideration. Finally, for a thin flat plate element can employ the shell element, when both bending and in plane movement are investigated. The formulation of structural intensity in the shell element is

$$\begin{aligned} I_x &= -(1/2)\,\mathrm{Re}\left[\tilde{N}_x\dot{\tilde{u}}^* + \tilde{N}_{xy}\dot{\tilde{v}}^* + \tilde{Q}_x\dot{\tilde{w}}^* + \tilde{M}_x\dot{\tilde{\theta}}_y^* - \tilde{M}_{xy}\dot{\tilde{\theta}}_x^*\right]; \\ I_y &= -(1/2)\,\mathrm{Re}\left[\tilde{N}_y\dot{\tilde{v}}^* + \tilde{N}_{yx}\dot{\tilde{u}}^* + \tilde{Q}_y\dot{\tilde{w}}^* - \tilde{M}_y\dot{\tilde{\theta}}_x^* + \tilde{M}_{yx}\dot{\tilde{\theta}}_y^*\right], \end{aligned} \tag{5}$$

where $\tilde{N}_x, \tilde{N}_y, \tilde{N}_{xy} = \tilde{N}_{yx}$ and $\tilde{Q}_x, \tilde{Q}_y$ are complex membrane and transverse shear forces per unit width of plate, respectively; $\tilde{M}_x, \tilde{M}_y$ and $\tilde{M}_{xy} = \tilde{M}_{yx}$ are complex bending and twisting moments per unit width of plate, respectively; $\dot{\tilde{u}}^*, \dot{\tilde{v}}^*, \dot{\tilde{w}}^*$ are complex conjugate of translational velocities in *x*, *y*, *z* directions; $\dot{\tilde{\theta}}_x^*, \dot{\tilde{\theta}}_y^*$ are complex conjugate of rotational velocities around *x* and *y* axis.

This formulation has been examined previously in rectangular plates and extended to cylindrical shells in present research. From the finite element method of curved shell, an approximation of the physical process rather than the mathematical problem is introduced to solve the difficulties concerning the influence of the shell's curvature. This approach based on the finite element method separates the continuously curved thin shell to a group of small flat thin elements, and every element allow use of shell finite elements when the size of the elements decreases and the convergence of results occurs. For the thin cylindrical shell, the Eq. (5) which is expressed under the rectangular coordinate system will be transformed from the rectangular to the cylindrical coordinate system. The formulation of structural intensity in the cylindrical shell is

$$\begin{aligned} I_x &= -(1/2)\,\mathrm{Re}\left[\tilde{N}_x\dot{\tilde{u}}^* + \tilde{N}_{x\theta}\dot{\tilde{v}}^* + \tilde{Q}_x\dot{\tilde{w}}^* + \tilde{M}_x\dot{\tilde{\theta}}_\theta^* - \tilde{M}_{x\theta}\dot{\tilde{\theta}}_x^*\right]; \\ I_\theta &= -(1/2)\,\mathrm{Re}\left[\tilde{N}_\theta\dot{\tilde{v}}^* + \tilde{N}_{\theta x}\dot{\tilde{u}}^* + \tilde{Q}_\theta\dot{\tilde{w}}^* - \tilde{M}_\theta\dot{\tilde{\theta}}_x^* + \tilde{M}_{\theta x}\dot{\tilde{\theta}}_\theta^*\right], \end{aligned} \tag{6}$$

where *x* denotes the axial direction and θ denotes the circumferential direction under the cylindrical coordinate system, other quantities correspond to forces, moments, translational and rotational velocities under the cylindrical coordinate system.

For the steady state vibration derive from a harmonically excited system at frequency ω, the velocities can be replaced by displacements by using the commonly adopted complex algebra.

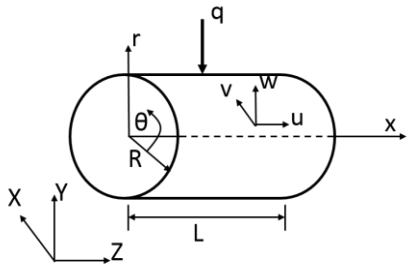

Fig. 2 Model of cylindrical shell and the definition of cylindrical coordinate

Therefore, the structural intensity for the steady vibrational cylindrical shell become

$$\begin{aligned} I_x &= -(\omega/2)\,\mathrm{Im}\left[\tilde{N}_x\tilde{u}^* + \tilde{N}_{x\theta}\tilde{v}^* + \tilde{Q}_x\dot{\tilde{w}}^* + \tilde{M}_x\tilde{\theta}_\theta^* - \tilde{M}_{x\theta}\tilde{\theta}_x^*\right]; \\ I_\theta &= -(\omega/2)\,\mathrm{Im}\left[\tilde{N}_\theta\tilde{v}^* + \tilde{N}_{\theta x}\tilde{u}^* + \tilde{Q}_\theta\tilde{w}^* - \tilde{M}_\theta\tilde{\theta}_x^* + \tilde{M}_{\theta x}\tilde{\theta}_\theta^*\right], \end{aligned} \tag{7}$$

where $\tilde{u}^*, \tilde{v}^*, \tilde{w}^*$ are complex conjugate of translational displacements in *x*, *y*, *z* directions; $\tilde{\theta}_x^*, \tilde{\theta}_y^*$ are complex conjugate of rotational displacements around *x* and *y* axis.

2.3 Displacement solution of vibrational cylindrical shells

In present study, the cylindrical shell model is assumed as elastic thin cylindrical shell and excited by a symmetrical harmonic transverse point force. The geometry and situation of load and support for the model is show in Fig. 2.

In order to calculate the structural intensity in this model, displacement fields and stress resultants should be obtained primarily. The material of this model is isotropic, elastic. The stress resultants are proportional to the spatial derivatives of the displacement fields. Therefore, the structural intensity can be expressed as the function of the displacement fields.

The displacement solution of this model through vibration theory is (Werner 1981)

$$\begin{aligned} u(x,\theta,t) &= \sum_{n=1}^{\infty} T_n(t)U_n(x,\theta); \\ v(x,\theta,t) &= \sum_{n=1}^{\infty} T_n(t)V_n(x,\theta); \\ w(x,\theta,t) &= \sum_{n=1}^{\infty} T_n(t)W_n(x,\theta), \end{aligned} \tag{8}$$

where *u*, *v*, *w* are displacement fields; U_n, V_n, W_n are displacement mode shapes; T_n is weight coefficient of time; *n* is the number of mode.

Under this special circumstance, the displacement solution Eq. (8) can be written as

$$\begin{aligned} u(x,\theta,t) &= \frac{2P_0}{\pi L\rho h}\sin\omega_0 t\sum_{m=1}^{\infty}\sum_{n=1}^{\infty}\frac{\bar{A}_{mn}}{\bar{A}_{mn}^2+\bar{B}_{mn}^2+1}\frac{\sin\frac{m\pi}{L}x_0\cos n\theta_0}{\omega_{mn}^2-\omega_0^2}\cos\frac{m\pi}{L}x\cos n\theta; \\ v(x,\theta,t) &= \frac{2P_0}{\pi L\rho h}\sin\omega_0 t\sum_{m=1}^{\infty}\sum_{n=1}^{\infty}\frac{\bar{B}_{imn}}{\bar{A}_{mn}^2+\bar{B}_{mn}^2+1}\frac{\sin\frac{m\pi}{L}x_0\cos n\theta_0}{\omega_{mn}^2-\omega_0^2}\sin\frac{m\pi}{L}x\sin n\theta; \\ w(x,\theta,t) &= \frac{2P_0}{\pi L\rho h}\sin\omega_0 t\sum_{m=1}^{\infty}\sum_{n=1}^{\infty}\frac{1}{\bar{A}_{mn}^2+\bar{B}_{mn}^2+1}\frac{\sin\frac{m\pi}{L}x_0\cos n\theta_0}{\omega_{mn}^2-\omega_0^2}\sin\frac{m\pi}{L}x\cos n\theta, \end{aligned} \tag{9}$$

where L and h are length and thickness of the cylindrical shell, respectively; ρ is mass density; P_0 and ω_0 are the amplitude and frequency of exciting force, respectively; m and n are wave number; $\bar{A}_{mn}, \bar{B}_{mn}$ are the ratio of displacement modes; ω_{mn} is modal frequency.

2.4 Formulation of structural intensity by vibration mode shapes

For the steady state vibration, the stress resultants and displacement fields can be expressed by quantities of vibration mode shapes. And the formulation of structural intensity can be expressed as following

$$\begin{aligned} I_x &= -(\omega_0/2)\left[\hat{N}_x\hat{u} + \hat{N}_{x\theta}\hat{v} + \hat{Q}_x\hat{w} + \hat{M}_x\hat{\theta}_x + \hat{M}_{x\theta}\hat{\theta}_\theta\right]; \\ I_\theta &= -(\omega_0/2)\left[\hat{N}_\theta\hat{v} + \hat{N}_{\theta x}\hat{u} + \hat{Q}_\theta\hat{w} + \hat{M}_\theta\hat{\theta}_\theta + \hat{M}_{\theta x}\hat{\theta}_x\right], \end{aligned} \tag{10}$$

where ˆ denotes quantities of vibration mode shapes.

The quantities of vibration mode shapes also can be written in more detail. Substituting the stress resultants and displacement fields into the formulation of structural intensity, the structural intensity in the model for can be defined as

$$\begin{aligned} I_x = &-\frac{\omega_0}{2}\frac{4P_0^2K}{\pi^2L^2\rho^2h^2}\sum_{m=1}^{\infty}\sum_{n=1}^{\infty}\sum_{r=1}^{\infty}\sum_{s=1}^{\infty}\frac{\sin\frac{m\pi}{L}x_0\cos n\theta_0}{\left(\bar{A}_{mn}^2+\bar{B}_{mn}^2+1\right)\left(\omega_{mn}^2-\omega_0^2\right)}\frac{\sin\frac{r\pi}{L}x_0\cos s\theta_0}{\left(\bar{A}_{rs}^2+\bar{B}_{rs}^2+1\right)\left(\omega_{rs}^2-\omega_0^2\right)}\times \\ &\left\{\begin{array}{l} \left(\frac{\nu}{R}+\frac{\nu n}{R}\bar{B}_{mn}-\frac{m\pi}{L}\bar{A}_{mn}\right)\bar{A}_{rs}\sin\frac{m\pi}{L}x\cos n\theta\cos\frac{r\pi}{L}x\cos s\theta+ \\ \frac{1-\nu}{2}\left(\frac{m\pi}{L}\bar{B}_{mn}-\frac{n}{R}\bar{A}_{mn}\right)\bar{B}_{rs}\cos\frac{m\pi}{L}x\sin n\theta\sin\frac{r\pi}{L}x\sin s\theta+ \\ kR^2\frac{m\pi}{L}\left[\left(\frac{n}{R}\right)^2+\left(\frac{m\pi}{L}\right)^2+\frac{1+\nu}{2}\frac{n}{R^2}\bar{B}_{mn}\right]\cos\frac{m\pi}{L}x\cos n\theta\sin\frac{r\pi}{L}x\cos s\theta- \\ kR^2\left[\nu\left(\frac{n}{R}\right)^2+\left(\frac{m\pi}{L}\right)^2+\frac{\nu n}{R^2}\bar{B}_{mn}\right]\frac{r\pi}{L}\cos\frac{m\pi}{L}x\cos n\theta\sin\frac{r\pi}{L}x\cos s\theta+ \\ k\frac{1-\nu}{2}\frac{m\pi}{L}\left(\bar{B}_{mn}+2n\right)\left(r+\bar{B}_{rs}\right)\cos\frac{m\pi}{L}x\sin n\theta\sin\frac{r\pi}{L}x\sin s\theta \end{array}\right\}; \\ I_\theta = &-\frac{\omega_0}{2}\frac{4P_0^2K}{\pi^2L^2\rho^2h^2}\sum_{m=1}^{\infty}\sum_{n=1}^{\infty}\sum_{r=1}^{\infty}\sum_{s=1}^{\infty}\frac{\sin\frac{m\pi}{L}x_0\cos n\theta_0}{\left(\bar{A}_{mn}^2+\bar{B}_{mn}^2+1\right)\left(\omega_{mn}^2-\omega_0^2\right)}\frac{\sin\frac{r\pi}{L}x_0\cos s\theta_0}{\left(\bar{A}_{rs}^2+\bar{B}_{rs}^2+1\right)\left(\omega_{rs}^2-\omega_0^2\right)}\times \\ &\left\{\begin{array}{l} \left(\frac{1}{R}+\frac{n}{R}\bar{B}_{mn}-\frac{\nu m\pi}{L}\bar{A}_{mn}\right)\bar{B}_{rs}\sin\frac{m\pi}{L}x\cos n\theta\sin\frac{r\pi}{L}x\sin s\theta+ \\ \frac{1-\nu}{2}\left(\frac{m\pi}{L}\bar{B}_{mn}-\frac{n}{R}\bar{A}_{mn}\right)\bar{A}_{rs}\cos\frac{m\pi}{L}x\sin n\theta\cos\frac{r\pi}{L}x\cos s\theta- \\ kR\left\{n\left[\left(\frac{n}{R}\right)^2+\left(\frac{m\pi}{L}\right)^2\right]+\left[\frac{1-\nu}{2}\left(\frac{m\pi}{L}\right)^2+\left(\frac{n}{R}\right)^2\right]\bar{B}_{mn}\right\}\sin\frac{m\pi}{L}x\sin n\theta\sin\frac{r\pi}{L}x\cos s\theta+ \\ kR\left[\left(\frac{n}{R}\right)^2+\nu\left(\frac{m\pi}{L}\right)^2+\frac{n}{R^2}\bar{B}_{mn}\right]\left(r+\bar{B}_{rs}\right)\sin\frac{m\pi}{L}x\cos n\theta\sin\frac{r\pi}{L}x\sin s\theta- \\ kR\frac{1-\nu}{2}\frac{m\pi}{L}\left(\bar{B}_{mn}+2n\right)\frac{r\pi}{L}\cos\frac{m\pi}{L}x\sin n\theta\cos\frac{r\pi}{L}x\cos s\theta \end{array}\right\}. \end{aligned} \tag{11}$$

The Eq. (11) shows that the structural intensity is an infinite weighted sum of function of vibration mode shapes. Simplify the detailed formulation to weight coefficients about load conditions and distribution functions of vibration mode shapes, the SI can be further expressed as

$$\begin{aligned} I_x &= -(\omega_0/2)C\sum_{m=1}^{\infty}\sum_{n=1}^{\infty}\sum_{r=1}^{\infty}\sum_{s=1}^{\infty} f_{mn}\cdot f_{rs}\cdot X_{mnrs}(x,\theta); \\ I_\theta &= -(\omega_0/2)C\sum_{m=1}^{\infty}\sum_{n=1}^{\infty}\sum_{r=1}^{\infty}\sum_{s=1}^{\infty} f_{mn}\cdot f_{rs}\cdot \Theta_{mnrs}(x,\theta), \end{aligned} \tag{12}$$

where C is model coefficient; $f_{mn} \cdot f_{rs}$ are weight coefficients; X_{mnrs}, Θ_{mnrs} are distribution functions; m, n, r, s are wave numbers. The wave numbers indicate the number of waves on the vibration shapes and represents a definite modal. The (m, n) mode means that there is m half waves in the axial direction of the vibrating cylindrical shell, and n waves in its circumferential direction. We use (m, n) to represent the modality of a force condition, using (r, s) for a displacement of the modal. Finally, the (m, n, r, s) can represent a modal state of the structural intensity component. In this equation, the weight coefficient components show the load conditions and reflect the weight coefficient of time. The distribution functions indicate the spatial derivative relationships between the stress resultants and displacement fields in structural intensity.

In the previous derivation, the range of sum is infinite and it is difficult to compute those equations. Therefore, the equations need to be approximated numerically in the numerical computation of the displacement fields or their time derivatives, and the number of modes which enter the analysis has to be appropriately chosen in such a way that the upper limit of frequency used in computation needs to be a few times higher than the excitation frequency.

For a certain number of mode, the weight coefficients and distribution functions can be obtained through Eq. (12). The results of distribution functions can reflect the pattern of structural intensity in specific mode and the weight coefficients decide the influence of this specific pattern on the sum range. As a result, an approach has been developed that a destination pattern of structural intensity can be reached approximately by enumerating distribution functions and selecting correct weight coefficients.

2.5 Structural intensity streamline presentation in cylindrical shells

The structural intensity in the thin cylindrical shell surface is expressed as a vector field, and the vector field can be visualized by a vectogram to provides the magnitude and direction distributions of structural intensity. However, to represent the trend of structural power flow in the cylindrical shell, the streamlines display technique should be employed.

Inspired by flow line concept in fluid mechanics, the structural intensity streamlines are a family of curves that are instantaneously tangent to the vector of the structural intensity. For steady vibration, the structural intensity streamlines are the vibrational power flow paths and allow to effectively assess vibrational sources and sinks. The same as fluid mechanics concept, the structural intensity streamlines can be defined as

$$\mathrm{d}\mathbf{r} \times \mathbf{I}(\mathbf{r}, t) = 0, \tag{13}$$

where $\mathbf{r}$ is particle position; $\mathbf{I}$ is structural intensity vector. The structural intensity vectors that located on the streamlines are perpendicular to $\mathbf{r}$ and parallel to d$\mathbf{r}$. For the cylindrical shell, the differential equation describing is

$$\frac{dx}{I_x} + \frac{Rd\theta}{I_\theta} = 0. \tag{14}$$

Every particular point that locate on the cylindrical shell corresponds with a structural intensity vector, and the vector is tangential to a streamline at this point. Therefore, the group of streamlines can describe the power flow travel paths on the cylindrical shell

2.6 Relationships between structural intensity and acoustic intensity

The energy governing equation can be derived by using three relationships: (a) a transmission equation relating energy density and intensity; (b) an energy balance equation from continuum mechanics; (c) an energy loss relationship where dissipated power is related to the local energy density in the vibrational medium using a loss factor. These three relationships are coupled to develop equations which govern the energy density in various vibrational systems.

An energy balance in an elastic medium can be described using a control volume approach. The flow of energy across any given closed surface is equivalent to the rate of change of the total energy inside the surface which encloses the volume (Bouthier and Bernhard 1995)

$$\int_V \frac{de}{dt} dV = \int_S \left(\sigma \cdot \frac{d\mathbf{u}}{dt} \right) d\mathbf{A} + \int_V \left(\pi_{in} - \pi_{diss} \right) dV, \tag{15}$$

where e is the energy density inside the control volume; **u** is the displacement vector of any particle on the boundary of the control volume; π_{in} is the input power density or energy input per unit volume per unit time; π_{diss} is the power density dissipated or energy per unit volume dissipated per unit time; d**A** is the vector normal to the surface of the control volume for a given point on the surface.

By using the divergence theorem and concept of structural intensity, the Eq. (15) can be rewritten as

$$\int_V \frac{de}{dt} dV = -\int_V \nabla \cdot I dV + \int_V \left(\pi_{in} - \pi_{diss} \right) dV. \tag{16}$$

And the integration limits in Eq. (16) are arbitrary, it becomes

$$\frac{de}{dt} = \pi_{in} - \pi_{diss} - \nabla \cdot I. \tag{17}$$

Eq. (17) is an energy balance relationship for all elastic media and is valid for steady or transient analysis. For vibro-acoustic case, the loading term is composed of internal driving force distribution density and external fluid loading. This model is excited by a transverse point force F_e and interacts with external fluid loading F_a , the input power flow density can be expressed as

$$\pi_{in} = F_e \left(\frac{d\mathbf{u}}{dt} \cdot \mathbf{n} \right) - F_a \left(\frac{d\mathbf{u}}{dt} \cdot \mathbf{n} \right). \tag{18}$$

Recognizing that the term of fluid loading is the normal component of the instantaneous acoustic intensity vector **J**, therefore Eq. (18) can be further expressed as

$$\pi_{in} = F_e \dot{w} - \mathbf{J} \cdot \mathbf{n}. \tag{19}$$

Substituting Eq. (19) into Eq. (17), the relationship between structural intensity and acoustic intensity can be obtained and expressed as

$$\frac{de}{dt} = F_e \dot{w} - \mathbf{J} \cdot \mathbf{n} - \pi_{diss} - \nabla \cdot I. \tag{20}$$

For the analysis of steady state vibrational energy propagation, all terms in Eq. (20) are time averaged over one cycle and the time variation of all energy is zero, then

$$\frac{de}{dt} = 0 = F_e \dot{w} - \mathbf{J} \cdot \mathbf{n} - \pi_{diss} - \nabla \cdot I. \tag{21}$$

Finally, the relationship between the acoustic density and the structural intensity and the changing power density that any power input by exciting force and loss from vibrating is obtained

$$\nabla \cdot I = F_e \dot{w} - \mathbf{J} \cdot \mathbf{n} - \pi_{diss}. \tag{22}$$

2.7 Analysis of structural acoustic coupling

Acoustic intensity is the sound energy which passes through a specific area at a certain point in the sound field in a specific time. Acoustic intensity at a point in the sound field in a specific direction r can be expressed as (Fahy and Gardonio 2007)

$$J = \frac{1}{2} p v^*, \tag{23}$$

where p and v are sound pressure and particle velocity; * denotes the complex conjugate.

The acoustic pressure field is related to the surface integral of the acoustic parameters over the surface of the structure of interest. For a harmonically vibrational cylindrical shell surface extending over an internal space, which the reflected sound is able to neglect, the acoustic pressure field can be described as

$$p(x, \theta, z) = \frac{jk\rho_0 c_0}{2\pi} \int_s \frac{v_n}{r} e^{j(\omega t - kr)} ds, \tag{24}$$

where p is the sound pressure at any field point; v_a is the normal velocity of the vibrational surface at any point; r is the distance between the two point; k is the acoustic wave number; ρ_0 and c_0 are density and sound velocity of air. Dividing the shell surface into curved elements and interpolating the structural normal velocity and surface pressure over each element allow Eq. (24) to be written in terms of the nodal normal velocity $\{v_n\}$ and surface pressure $\{p\}$ as

$$\{p\} = [D]\{v_n\}, \tag{25}$$

where $[D]$ is the acoustic impedance matrix.

In the previous part, the acoustic intensity is recognized as the term of fluid loading. Therefore, the acoustic intensity in the vibrational cylindrical shell surface can be further written as

$$\mathbf{J} = F_a \cdot \frac{d\mathbf{u}}{dt}, \tag{26}$$

This equation provides the contact between the sound pressure and normal velocity on the plate surface. In order to further investigate the coupling relation between structural intensity and acoustic intensity, the two expressions are compared and some similarities are obtained as follow. For flexural wave motion in shell structure, the bending moment energy contribution is the main component of structural intensity, and acoustic intensity is significantly affected by bending motion. In the case of interaction between vibrational shell and air medium, both structural intensity and acoustic intensity can reflect the level of vibration. Therefore, in some conditions, the

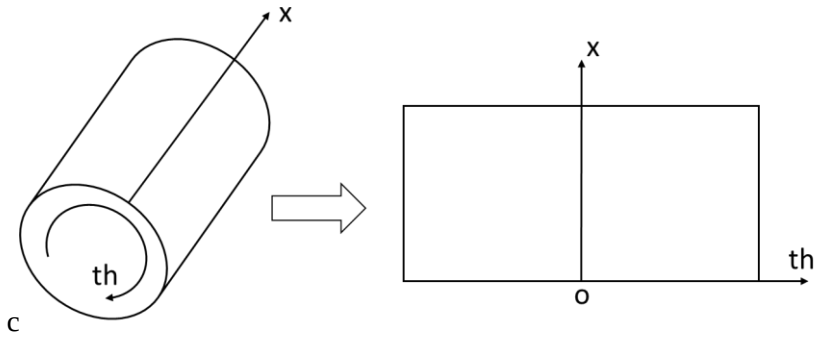

Fig. 3 The mapping procedure

Table 1 Geometrical model and materials properties of structure and air

Length	10 m	Model density	2618 kg·m^{-3}
Radius	3 m	Young modulus	72.4 MPa
Thickness	0.1 m	Air density	1.2 kg·m^{-3}
Poisson's ratio	0.33	Speed of sound in air	343 m·s^{-1}

change trend of acoustic intensity is similar to structural intensity.

3. Analytical solution and numerical simulation

3.1 The structural intensity calculation

In this section, the structural intensity of a cylindrical shell under steady excitation is calculated by theoretical analyses and numerical simulation. This cylindrical shell structure which consists of an aluminum open cylindrical shell with a 0.10 m thickness and surrounded by air circumstance is excited by a symmetrical harmonic normal point force. Fig. 2 shows the geometry of the structure and the coordinate system in the analysis. The materials properties and main geometrical parameters of the cylindrical shell are represented in Table 1. According to previous derived formulations, the MATLAB programs are used for calculation. In the analyses, the amplitude of excitation is 1000N and frequencies of excitation are selected as follow: 100rad·s^{-1}, 210rad·s^{-1} and 250rad·s^{-1}. To clearly visualize the results, we transform the cylindrical shell results into a two-dimensional plane. In the transformed form, the excitation position is the center of the two-dimensional plane. The mapping procedure is shown in Fig. 3. And the structural intensity streamline maps of the cylindrical shell under series excitations are given in Fig. 4. From Fig. 4 it can be found that the results are different under different excitations. Comparing three figures in Fig. 4, we can find that Fig. 4(b) is the most regular pattern. Meanwhile, the excitation frequency of Fig. 4(b) is closest to the natural frequency of (1, 3) mode (210.86 rad·s^{-1}).

3.2 Control method of structural intensity

Based on the former theoretical analysis, structural intensity distribution is mainly affected by

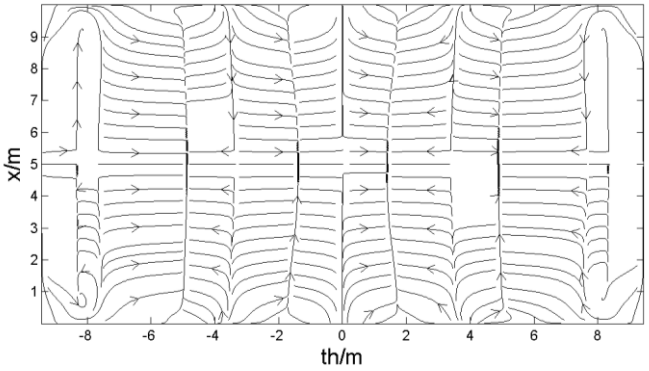

(a) Excitation frequency 100 rad·s^{-1}

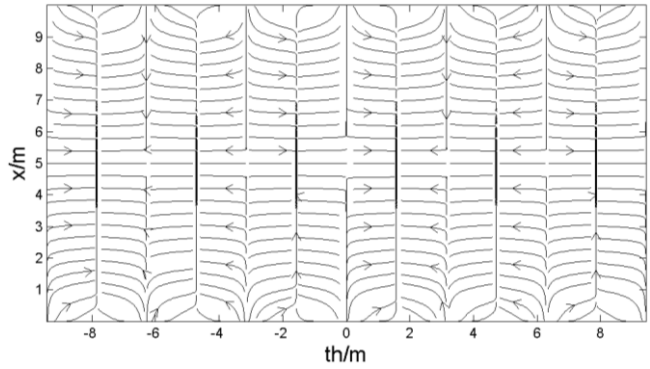

(b) Excitation frequency 210 rad·s^{-1}

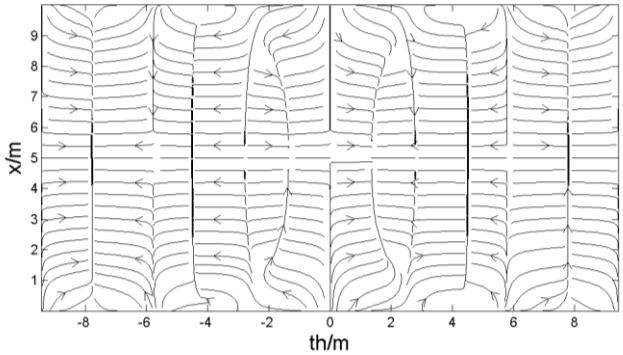

(c) Excitation frequency 250 rad·s^{-1}

Fig. 4 Streamline maps of structural intensity of cylindrical shell at 2-D plan view

weight coefficients $f_{mn} \cdot f_{rs}$ and distribution functions X_{mnrs}, Θ_{mnrs}. Distribution functions decide the pattern of structural intensity on cylindrical shell at any (m, n, r, s) mode, while weight coefficients determine the proportion of corresponding mode pattern in total structural intensity.

Distribution functions are mostly related to structural vibrational mode. The distribution functions for each mode is determined and the streamline maps of the distribution functions for several modes are shown in Fig. 5. From Fig. 5, it can be observed that the streamline map of structural intensity at exciting frequency of 210 rad·s^{-1} (as shown in Fig. 4(b)) is almost the same as the streamline pattern of distribution functions in Fig. 5(a), where mode is (1, 3, 1, 3). Therefore, the

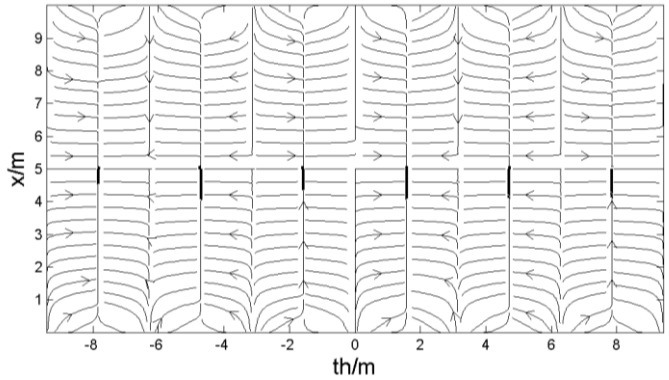

(a) (1,3,1,3) mode

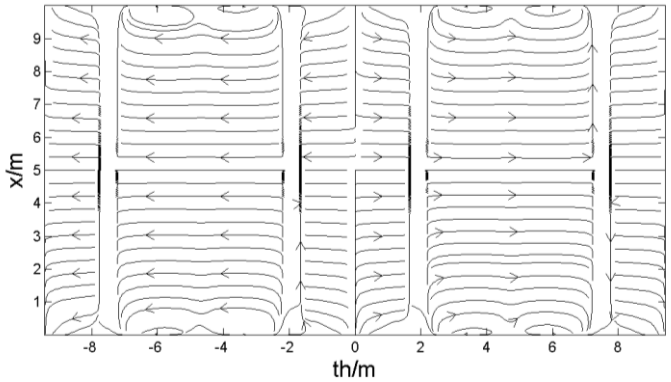

(b) (1,3,1,4) mode

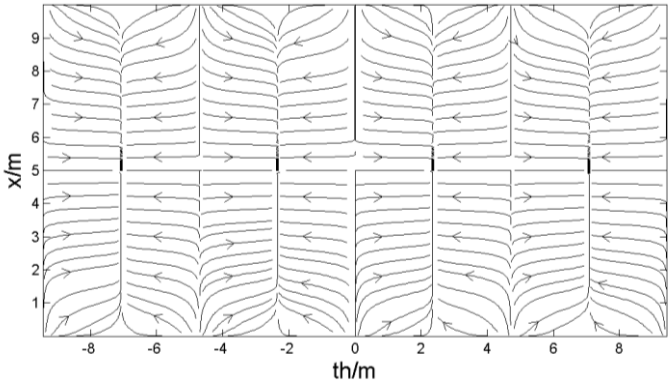

(c) (1,2,1,2) mode

Fig. 5 Streamline maps of distribution functions

structural intensity map at 210 rad·s^{-1} exciting frequency is mainly contributed by the distribution functions at (1, 3, 1, 3) mode. The magnitude of contribution is decided by weight coefficients and the formula of them shows that weight coefficients are affected by exciting frequency and position.

When the streamline patterns of distribution functions at certain modes are obtained, we can calculate the change curves of weight coefficients with the exciting frequency. The curves based on the value of weight coefficients under various exciting frequency, are shown in Fig. 6. It is

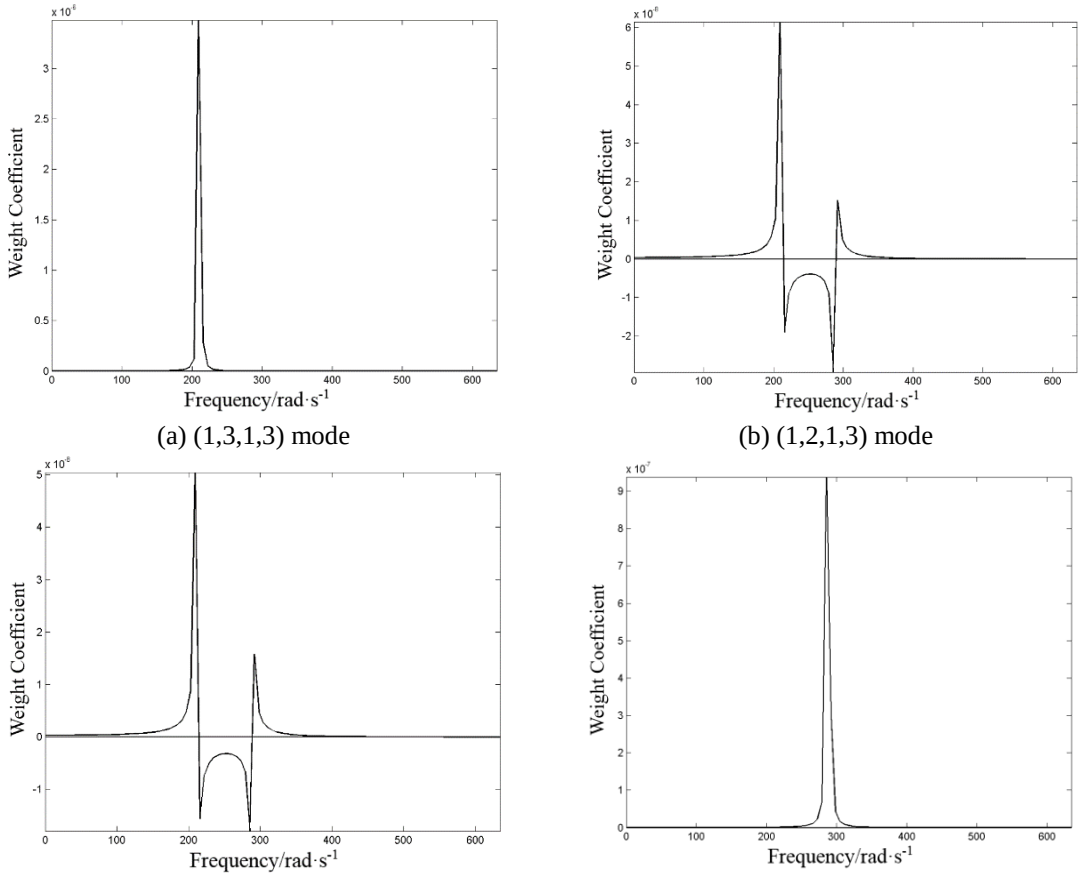

(a) (1,3,1,3) mode (b) (1,2,1,3) mode

(c) (1,3,1,4) mode (d) (1,2,1,2) mode

Fig. 6 Weight coefficients in different conditions

found that, when exciting frequency is close to a natural frequency, the weight coefficients reach their peak of the mode. Figs. 6(a)-(d) show the peak of main mode (1, 3, 1, 3) and (1, 2, 1, 2) of distribution functions when exciting frequencies are close to mode (1.3) and (1.2). Whereas the weight coefficients of minor modes (1, 2, 1, 3) and (1, 3, 1, 4) reach their peak and correspond to natural frequency of the modes (1, 2), (1, 3) and (1, 3), (1, 4), but far much smaller than the figure of weight coefficients in main mode. In the process, main mode is referring to m=r, n=s in mode targets (m, n, r, s), while minor modes refer to the others.

It represents that when exciting frequency is close to a natural frequency, the weight coefficient of this main mode reaches the peak, because of resonance phenomenon. Thus, it reveals why the streamline map of structural intensity is similar to pattern of distribution functions of the main mode. According to this, when exciting frequency is at 210 rad·s-1, due to its closeness with (1, 3) mode frequency (210.86 rad·s-1), its weight coefficients of main mode (1, 3, 1, 3) reach the peak. Then leads to a larger proportion of distribution functions pattern of main mode (1, 3, 1, 3) in structural intensity map, as shown in Fig. 5(a) and 4(b).

The influence of weight coefficients by the position of excitation can be analyzed by drawing the contour of weight coefficients on the cylindrical shell, as shown in Fig. 7; the different shades

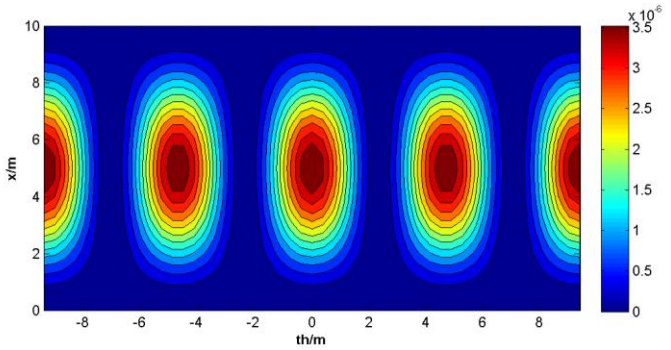

(a) (1,2,1,2) mode

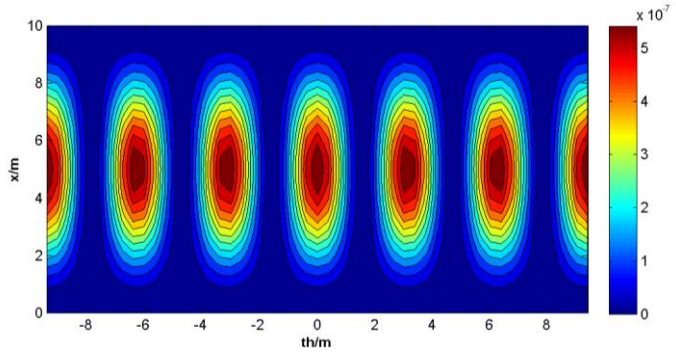

(b) (1,3,1,3) mode

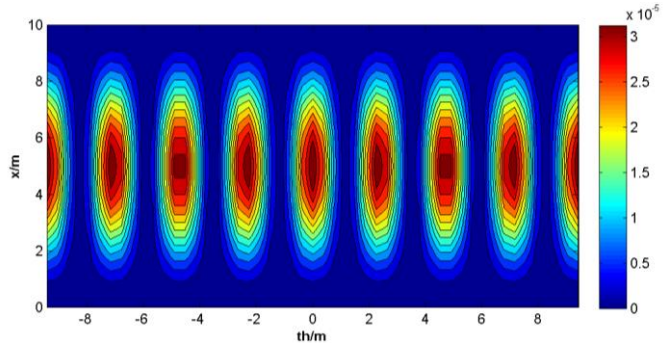

(c) (1,4,1,4) mode

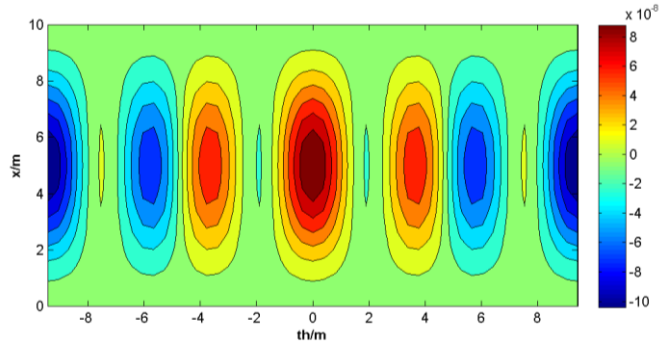

(d) (1,2,1,3) mode

Fig. 7 The contour of weight coefficients on the cylindrical shell

Table 2 Vibration modes and the modal frequencies of the cylindrical shell

Mode	Frequency/Hz	Mode	Frequency/Hz
(1, 3)	45.75	(2, 4)	77.45
(1, 4)	50.77	(2, 5)	87.37
(1, 2)	63.27	(2, 3)	88.46
(1, 5)	71.27	(1, 6)	100.47

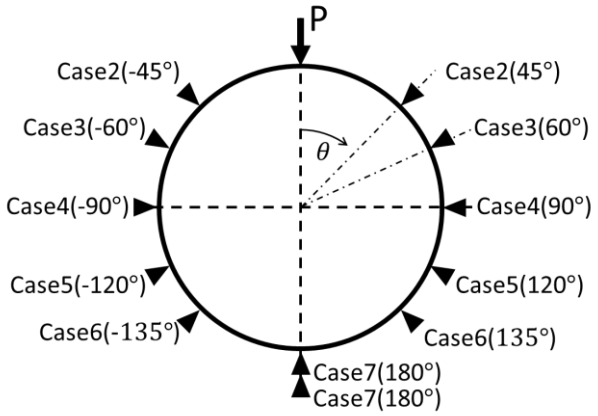

Fig. 8 Damping position on the cylindrical shell

of color illustrate the magnitude of weight coefficients at that exciting point. The contours show that the weight coefficient distribution on the cylindrical shell is correlated with normal displacement of vibration modes. As presented in Fig. 7(a), the contour is correlated with the (1, 2) mode on the cylindrical shell. Besides, weight coefficients corresponding to minor mode are far smaller than the one corresponding with main mode, as shown in Fig. 7(d).

Based on the former analysis, a design method of structural intensity distribution is presented. Firstly, calculating distribution functions of several main modes, and finding the main mode of desired structural intensity distribution. Selecting excitation frequency and position corresponding to the main mode. Then structural intensity distribution will be resulted by exciting the vibration on certain point. If desired structural intensity distribution has no directly corresponding main mode, the data can be calculated by using superposition principle. In former research, it's pointed out that redistribution of structural intensity can be done by changing exciting frequency and position, but the mechanism behind had not been explored. The mechanism of how to alter redistribution of structural intensity is given based on the formulation of structural intensity on the cylindrical shell and the formulation of its weight coefficients and distribution functions.

4. Application example for structural intensity approach

4.1 Simulation of the cylindrical shell

The vibro-acoustic behavior of a cylindrical shell, which represents the fuselage structure, is

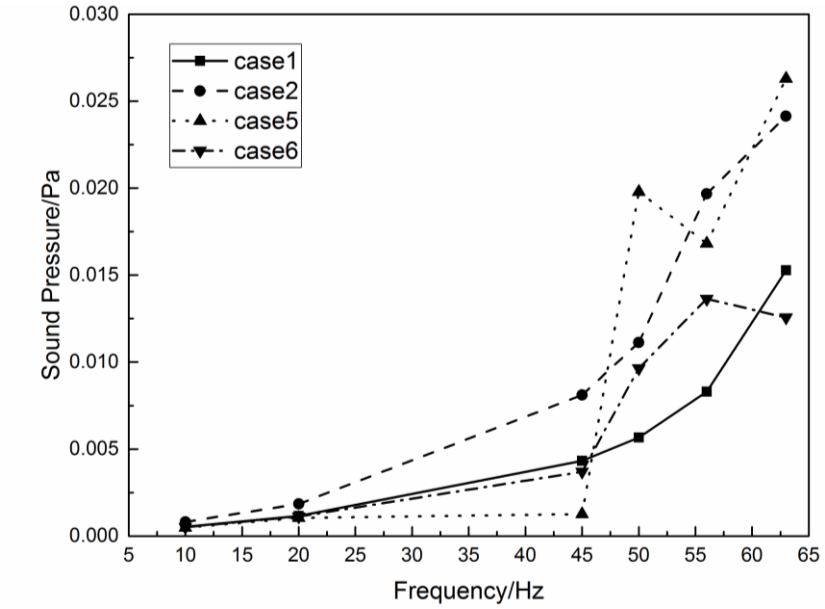

Fig. 9 The interior sound pressure frequency response for different damping cases

carried out by using finite element method and proposed SI approach. In this simulation, a COMSOL Multi-physics is used to simulate the structure vibration and vibro-acoustics. The structural intensity of the cylindrical shell structure is computed based on the formulations presented in Section 2.

Table 2 shows the vibration modes and their modal frequencies in the frequency range up to 100 Hz. The comparison of the simulation results and SI method for reducing noise level demonstrated that the proposed SI method is feasible and the results are reasonable.

Based on the natural frequencies, we use the following three conditions to select excitation frequencies: (a) below the first order natural frequency; (b) near the first order natural frequency; (c) between the first two order natural frequencies. The excitation frequencies are as follows: 10 Hz, 20 Hz, 45 Hz, 50 Hz, 56 Hz, 63 Hz, 71 Hz, 74 Hz and 77 Hz.

4.2 Damping properties of cylindrical shell

Referring to the vibrating shapes of the cylindrical shell, we symmetrically put two dampers on the structural surface in every case, except for case 1 without damping. Damping factor is selected to be 107 $Ns \cdot m^{-1}$. The positions of two dampers from case 2 to case 7 are shown in Fig. 8. These positions are near the extremes of transverse displacement in first few order vibrating shapes. Therefore, the displacement fields will be influenced by dampers in different case.

4.3 Sound pressure of central point

The central point of cylindrical shell is selected to be objective position. The data of internal sound at objective point in the model is obtained by simulation for different excitation frequency and damping cases. The sound pressures of objective point are shown in Fig. 9 for the case 1, case

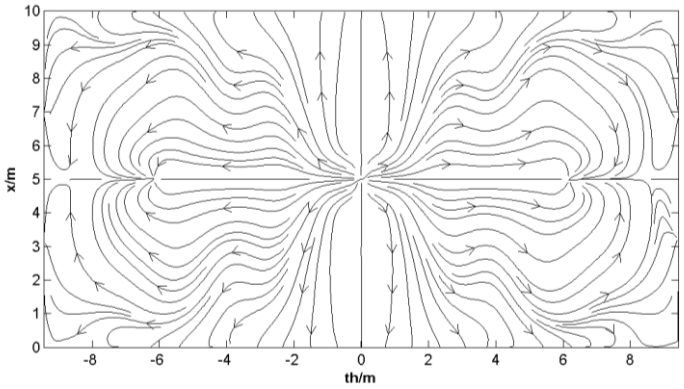

(a) For case 5 damping

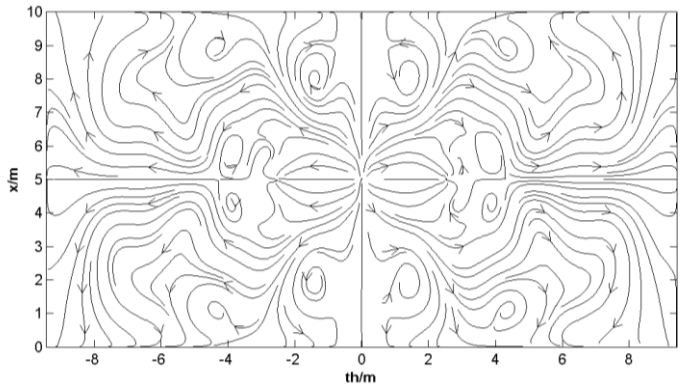

(b) For case 2 damping

Fig. 10 The structural intensity streamline map in excitation frequency 45 Hz

2, case 5 and case 6. From Fig. 9, it can be seen that the trend of sound pressure at central point with excitation frequency varies for different damping cases.

In the following, the relationship between structural intensity and internal sound field will be analyzed. It is because the changing place of damper in cases also changed the structural intensity distribution, thus affected the central sound pressure. Take 45 Hz excitation frequency for example, the low sound pressure in case 5 and high one in case 2 of streamline maps are shown in Fig. 10, it can be seen that the sources and sink are identified. The direction of structural intensity flow is clear for case 5, where most of the streamlines can be linked from the source to sink. However, there are many eddies for case 2, and only few streamlines flow from source to sink, which means damper doesn't have much effects. These eddies pattern have the potential of confining the structural power flow into a specific area of the structure.

Analyzing from the vibration mode, normal displacement vibration mode of no-damper case and in case 5 are shown in Fig. 11 respectively. Since the excitation frequency of 45 Hz is close to natural frequency at (1, 3) mode, these two dampers in case 5 are placed coincidently around the maximum point, thus reduced the vibration amplitude efficiently and lead to the reduction of vibro-acoustic energy.

Through preceding text comparison, it is found that the sound pressure response curve at objective point changed in different cases. Therefore, the internal sound field in vibrating

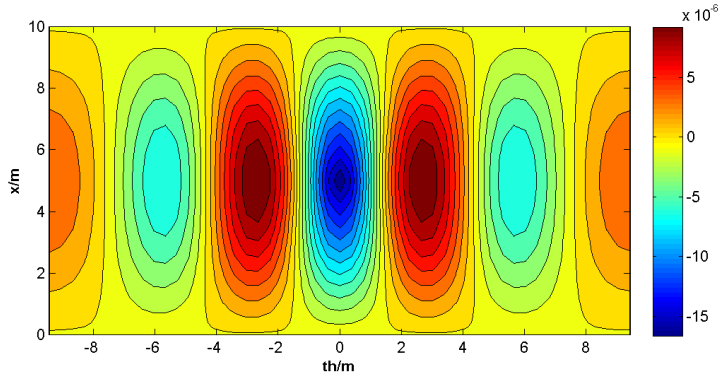

(a) No-damper case

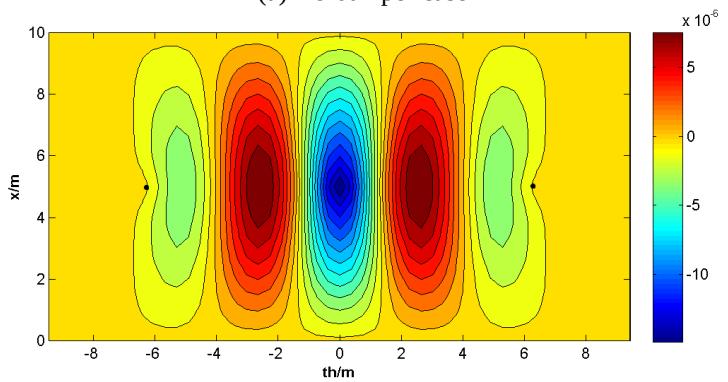

(b) For case 5 damping

Fig. 11 The normal displacement in excitation frequency 45 Hz

cylindrical shell is changing with different structural intensity distribution. In effect, the changing of vibration shape affects the internal sound field, and structural intensity distribution can reflect this changing in vibration shape.

4.4 Energy relationship between structural intensity and acoustic intensity

From the energy aspect, if loop-integration of structural intensity is applied on the inner surface of vibrating cylindrical shell, which is the coupling surface of vibration and sound, structural intensity energy can be obtained; and at mean time if the volume integral of internal acoustic intensity is used as sound energy, the changing pattern between structural intensity energy and sound energy under different excitation frequency can be discovered.

Structural intensity energy and sound energy profiles with different damping cases are shown in Fig. 12 for excitation frequencies of 20 Hz and 56Hz. According to the energy relationship for 20 Hz and 56 Hz excitation cases, we can find that although these two physical quantities represent the vibration of cylindrical shell and its internal sound field characteristic, their changing tendencies are almost the same while the damping condition is changed. Thus, if structural intensity energy can be reduced, sound energy of radiation can decrease, the sound energy of internal sound field also can be reduced. In short, the tendency of radiation sound energy can be predicted directly by monitoring the tendency of structural intensity energy.

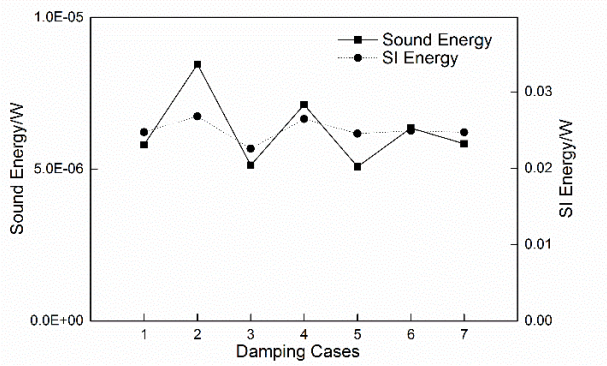

(a) Excitation frequency 20 Hz

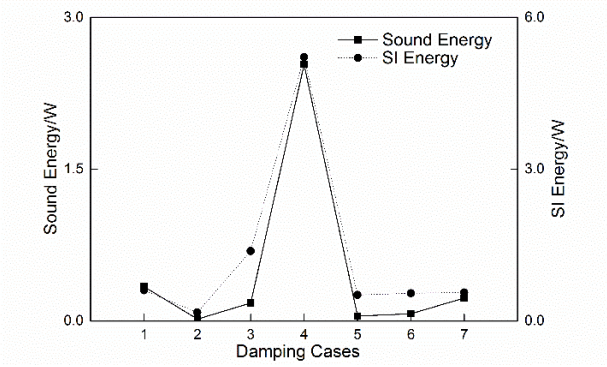

(b) Excitation frequency 56 Hz

Fig. 12 Structural intensity and sound energy trends in various cases

4.5 Sound control in the cylinder shell

According to previous analysis, reducing sound energy in sound field can be obtained by decreasing the structural intensity energy. By observing the distribution of structural intensity, we can find the collecting point of energy and place dampers to create a sink. These points can significantly absorb energy in structure.

Take 50 Hz excitation frequency for example, the SI streamline map with and without damper are shown in Fig. 13. There are some eddies formed by streamline, and a damper is set at th= -4.7 m, x=2.0 m in the eddy, thus a new distribution of streamlines is created and shown in Fig. 13(b). It is shown that the eddy is replaced by a sink, and all the streamlines are pointed to the sink where energy can flow into specific area.

The structural intensity contours for excitation frequency at 50 Hz with and without damper are shown in Fig. 14 respectively. By comparing the amplitude of structural intensity between two cases, reducing structural intensity level can be obtained by setting damper in the particular position. The before and after calculations of structural intensity energy and acoustic energy in selected objective point are shown in Table 3. Compared with no-damper situation, structural intensity energy and acoustic energy are reduced significantly. Other cases also got the similar results. In general, reducing structural intensity energy and radiation acoustic energy in objective point can be reached through properly placing dampers at eddies formed by streamlines.

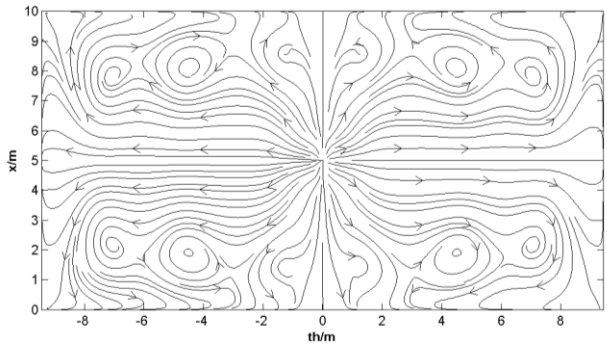

(a) No damper

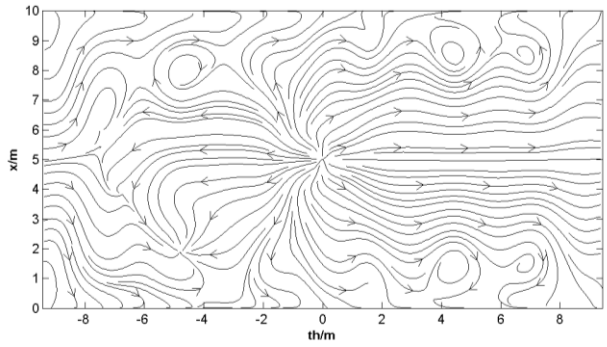

(b) With damper

Fig. 13 The structural intensity streamline map in excitation frequency 50 Hz

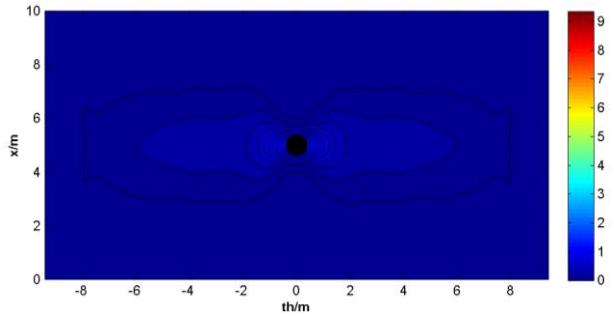

(a) No damper

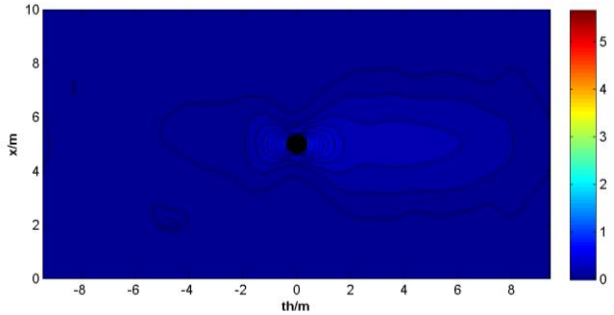

(b) With damper

Fig. 14 The structural intensity contour in excitation frequency 50 Hz

Table 3 Comparison of energy changing by setting damper

	Structural intensity energy/W	Sound energy/W
No damper	3.7522	0.05525
With damper	2.1517	0.03488

5. Conclusions

Through theoretical analyses and modeling simulation for the coupling vibration and acoustical radiation problem, the relationship between vibro-acoustic energy and structural intensity distribution of the cylindrical shell is derived. First, the structural intensity method has been adopted to evaluate the vibrations of a cylinder shell. Then, according to derived relationship of structural intensity and vibration and acoustic energy for cylindrical shell structure, we proposed an approach of changing vibro-acoustic properties by altering structural intensity. In the study, the structural intensity streamlines method, which can be used to clearly indicate the source, the sink and the direction of power flow paths from the source to the sink of the structures, are adopted.

From present study, we find that the internal acoustic pressure field has the close connection with structural intensity in the interface of structural-acoustic coupling. From the energy aspect, this work computes loop-integration of structural intensity and volume-integral of internal acoustic intensity and defines these integral respectively as structural intensity energy and sound energy. These energy in different damping-cases and exaction frequencies are calculated. Comparing the results, we discover that the trend of these energy change is similar in same cases. It can be concluded that the control of the sound radiation energy for a vibrating structure can be achieved by changing the structural intensity energy.

Furthermore, a method which can reduces the acoustic energy through properly putting damper position and redistributing the structural intensity in the cylinder shell is developed. For cylinder shell structures, there are some eddies pattern in the structural intensity streamline, and these eddies have potential of collecting energy. When the damper is put in the eddy position, the stored energy will be released and a new sink appears. According to source and sink positions, we can modify the structural intensity distribution so as to reduce the acoustic energy of cylinder shell structure.

Acknowledgments

Authors are grateful for the support from the National Natural Science Foundation of China through grant numbers 11372236, 11572236 and 11321062.

References

Alfredsson, K.S. (1993), "Influence of local damping on active and reactive power flow", *Proceedings of the International Congress on Intensity Techniques*, Sep.

Audrain, P., Masson, P., Berry, A., Pascal, J.C. and Gazengel, B. (2004), "The use of PVDF strain sensing in active control of structural intensity in beams", *J. Intellig. Mater. Syst. Struct.*, **15**(5), 319-327.

Bouthier, O.M. and Bernhard, R.J. (1995), "Simple models of the energetics of transversely vibrating plates", *J. Sound Vibr.*, **182**(1), 149-164.

Chesnais, C., Totaro, N., Thomas, J.H. and Guyader, J.L. (2017), "Reconstruction and separation of

vibratory field using structural holography", *J. Sound Vibr.*, **389**, 134-152.
Fahy, F. and Gardonio, P. (2007), *Sound and Structural Vibration: Radiation, Transmission and Response: Second Edition*, Academic Press.
Gavrić, L. and Pavić, G. (1993), "A finite element method for computation of structural intensity by the normal mode approach", *J. Sound Vibr.*, **164**(1), 29-43.
Gavrić, L., Carlsson, U. and Feng, L. (1997), "Measurement of structural intensity using a normal mode approach", *J. Sound Vibr.*, **206**(1), 87-101.
Hambric, S.A. (1990), "Power flow and mechanical intensity calculations in structural finite element analysis", *J. Vibr. Acoust.*, **112**(4), 542-549.
Huang, Y.M. and Chen, C.C. (2000), "Optimal design of dynamic absorbers on vibration and noise control of the fuselage", *Comput. Struct.*, **76**(6), 691-702.
Huang, Y.M. and Tseng, H.C. (2008), "Active piezoelectric dynamic absorbers on vibration and noise reductions of the fuselage", *J. Mech.*, **24**(1), 69-77.
Javed, S., Viswanathan, K.K. and Aziz, Z.A. (2016), "Free vibration analysis of composite cylindrical shells with non-uniform thickness walls", *Steel Compos. Struct.*, **20**(5), 1087-1102.
Li, Y.J. and Lai, J.C.S. (2000), "Prediction of surface mobility of a finite plate with uniform force excitation by structural intensity", *Appl. Acoust.*, **60**(3), 371-383.
Liu, Z.S., Lee, H.P. and Lu, C. (2006), "Passive and active interior noise control of box structures using the structural intensity method", *Appli. Acoust.*, **67**(2), 112-134.
Liu, Z.S., Lee, H.P. and Lu, C. (2005), "Structural intensity study of plates under low-velocity impact", *Int. J. Imp. Eng.*, **31**(8), 957-975.
Liu, Z.S., Luo, X.Y., Lee, H.P. and Lu, C. (2007), "Snoring source identification and snoring noise prediction", *J. Biomech.*, **40**(4), 861-870.
Liu, Z.S., Swaddiwudhipong, S., Lu, C. and Hua, J. (2005), "Transient energy flow in ship plate and shell structures under low velocity impact", *Struct. Eng. Mech.*, **20**(4), 451-463.
Noiseux, D.U. (1970), "Measurement of power flow in uniform beams and plates", *J. Acoust. Soc. Am.*, **47**(1B), 238-247.
Pavić, G. (1976), "Measurement of structure borne wave intensity, part I: Formulation of the methods", *J. Sound Vibr.*, **49**(2), 221-230.
Verheij, J.W. (1980), "Cross spectral density methods for measuring structure borne power flow on beams and pipes", *J. Sound Vibr.*, **70**(1), 133-138.
Wang, J., Zhang, C., Wu, Z., Wharton, J. and Ren, L. (2017), "Numerical study on reduction of aerodynamic noise around an airfoil with biomimetic structures", *J. Sound Vibr.*, **394**, 46-58.
Wang, D.F., He, P.F. and Liu, Z.S. (2005), *Structural Intensity of Cylindrical Shell Structure under Dynamic Loading*, ISISS 2005: Innovation & Sustainability of Structures.
Williams, E.G. (1991), "Structural intensity in thin cylindrical shells", *J. Acoust. Soc. Am.*, **89**(4), 1615-1622.
Werner, S. (1981), *Vibrations of Shells and Plates*, CRC Press.
Wu, S.F. and Zhou, P. (2016), "Analyzing excitation forces acting on a plate based on measured acoustic pressure", *J. Acoust. Soc. Am.*, **140**(1), 510-523.
Sommerfeldt, S.D. (1993), "Active vibration control using structural intensity", *J. Acoust. Soc. Am.*, **93**(4), 2370-2370.
Thompson, A.G. (1989), "The effect of tyre damping on the performance of vibration absorbers in an active suspension", *J. Sound Vibr.*, **133**(3), 457-465.
Xu, X.D., Lee, H.P., Lu, C. and Guo, J.Y. (2005), "Streamline representation for structural intensity fields", *J. Sound Vibr.*, **280**(1), 449-454.
Zhao, C., Wang, P. and Yi, Q. (2017), "Internal noise reduction in railway vehicles by means of rail grinding and rail dampers", *Noise Contr. Eng. J.*, **65**(1), 1-13.